R. & M. No. 3809

R. & M. No. 3809

PROCUREMENT EXECUTIVE, MINISTRY OF DEFENCE

AERONAUTICAL RESEARCH COUNCIL
REPORTS AND MEMORANDA

Flight Measurements of the Effects of Simulated Leading-Edge Erosion on Helicopter Blade Stall, Torsional Loads and Performance

By P. BROTHERHOOD and D. W. BROWN

Structures Department, R.A.E., Bedford

LONDON: HER MAJESTY'S STATIONERY OFFICE
1978
£3·50 net

Flight Measurements of the Effects of Simulated Leading-Edge Erosion on Helicopter Blade Stall, Torsional Loads and Performance

By P. BROTHERHOOD and D. W. BROWN

Structures Department, R.A.E., Bedford

Reports and Memoranda No. 3809*
March, 1976

Summary

The leading edges of the main rotor blades of a *Wessex* helicopter were artificially roughened to simulate light to moderate erosion of unprotected light alloy blades. Pitch link loads were measured in forward flight for various spanwise extents of leading-edge roughness, and the values of forward speed at which a pre-set limit of oscillatory pitch link load was reached were determined. This limit was set so as to avoid excessive fatigue damage to the modified control linkage. With a representative length of roughness, the speed at which the limit load occurred was reduced by 24 kn. This marked reduction was associated with premature blade stall, detected by trailing edge pressure measurements, and subsequent stall flutter together with an increased power requirement.

* Replaces R.A.E. TR 76039—A.R.C. 37 053

LIST OF CONTENTS

1. Introduction

Unprotected light alloy blades are particularly prone to erosion from exposure to heavy rain and sea spray. Erosion of this type is shown in Fig. 1 for unprotected *Wessex* and *Sea King* blades. It is most severe at the extreme tips and progressively lessens inboard, the effective area being a band about two to three centimetres wide around the leading edge and some one metre in length. The level of erosion depicted would be unacceptable in practice, and remedial measures (dressing out) would be necessary. The adverse effect of erosion is now appreciated and special protection is applied to the blades. Normally *Wessex* and *Sea King* blades are protected with a renewable polyurethane leading-edge strip which reduces the rate of erosion considerably even in extreme conditions. However, this does not provide a satisfactory level of protection against sand. Sand can also erode blades with stainless steel leading edges, although these are much less susceptible to rain erosion. Surface deterioration may therefore eventually occur in some degree even with protected light alloy or steel blades and the object of the tests described was to examine the effect in a controlled way using artificially roughened blades.

It is known from steady two-dimensional wind-tunnel tests that leading-edge roughness can lead to premature stall, and that stall produces a sudden and large change in pitching moment. Furthermore, two-dimensional wind-tunnel tests on oscillating aerofoils[1] have shown that negative damping and the tendency for stall flutter increases when leading-edge roughness is added. Thus, if a rotor is designed to operate in conditions close to the stall boundary, then any deterioration of the blade leading-edge surface might lead to stall flutter in conditions when it did not previously occur, resulting in a large increase in oscillatory torsional loads and fatigue damage; alternatively, if fatigue damage is to be avoided, then a reduction in forward speed must be accepted.

It is clearly essential, in any investigation of the effects of leading-edge erosion, to measure loads in the pitch link rods which effect the cyclic pitch change at the blade root and transmit torsional loads back to the control system via the swash plate. The availability of a *Wessex* helicopter, with a main rotor slip ring assembly through which measured blade parameters could be transmitted to the fuselage, suggested that some tests to investigate the gross effects of erosion could be made fairly quickly. This helicopter also had pitch link rods that had already been modified to incorporate strain gauges for the measurement of pitch link loads. In addition, it was decided that some indication of blade stall would be useful in explaining changes in pitch link load and the technique of monitoring trailing-edge pressure[2] was adopted. This technique had previously been used in flight[3] with divergence of trailing-edge pressure being associated with the onset of blade stall. Only one degree of roughness was used in the tests, representing slight to moderate erosion of unprotected light alloy blades, but the spanwise extent was varied in three stages in addition to datum tests with unroughened blades.

The tests were carried out at R.A.E., Bedford during May to July 1973.

2. Provision of Simulated Roughness

The eroded surface of unprotected light alloy blades (Fig. 1) consists of overlapping impacted cavities with scattered peaks and ridges, the whole area having a very rough granular quality; there is also some deformation of the profile itself. The latter effect was not simulated during the present tests: inspection of eroded blades shows it to be secondary to the primary characteristic of roughness.

In the present tests the roughness was simulated by gluing silicon carbide grit to the leading edge of the blade. The grains are coarse and angular and in order to select an appropriate grade, grits of various size were glued on to a test surface. The ratio of grit to treated area was approximately one half. By visual comparison and by running a finger over the surfaces a person experienced in assessing erosion during operational flying suggested No. 60 grit (subsequent sieving revealed a composition 0·29 mm, 60 per cent and 0·25 mm, 40 per cent i.e. a grain size of approximately 0·064 per cent of the blade chord) to be representative of small to moderate erosion. Various methods of sticking the grit to the blade were tried and the one finally chosen was to apply 25 mm Sellotape to the leading edge of the blade. This was then coated with quick-setting epoxy resin and the grit applied at the required density by hand. In this way the rough texture of the grit was maintained and not excessively reduced by immersion in the adhesive which still had sufficient grip to ensure minimal loss at the relatively high air speed of the blade tip. It was also possible to remove the roughness quickly and quite easily without damage to the blade by peeling off the Sellotape. Care was taken to avoid an abrupt edge to the roughness which was dressed where necessary.

It should be noted that the roughness was applied to the surface of the anti-erosion strip which is now standard on *Wessex* blades and which was in an almost unmarked condition on the test helicopter.

The extent of the roughness and its condition before and after the test series are shown in Fig. 2.

3. Instrumentation

The test aircraft had been used for general aerodynamic research for the past few years and the comprehensive instrumentation included a main rotor slip ring assembly. The relevant quantities recorded in the aircraft during the present tests using a 30 cm paper recorder are given below together with notes on method of measurement.

Airspeed: standard aircraft pitot-static source.
Normal acceleration.
Main rotor shaft torque: strain gauged rotor shaft.
Rotor blade azimuth position: electro magnetic pick-up on rotor shaft.
Pitch link load: specially modified and strain gauged pitch link, the output from one blade only was recorded.
Trailing edge pressure: a miniature semi-conductor absolute pressure transducer in a small protective case ($9 \times 12 \times 1{\cdot}5$ mm thick) was mounted on and faired into the upper surface of one blade at 0·91 rotor radius and 0·91 chord (Fig. 2). Connecting wires were run down the quarter chord line on the under surface to the slip rings forming a faired projection of 0·25 mm (blade chord 420 mm).

In addition to recording the pitch link load signal in the aircraft, it was also transmitted to the ground station by telemetry. There it was recorded and continuously monitored by an observer in radio contact with the pilot, who was immediately alerted should critical pitch link loads be reached.

4. Indication of Separated Flow from Measurements of Trailing-Edge Pressure Divergence

The use of upper surface pressure near the trailing edge of an aerofoil to indicate flow separation and stall is described in Ref. 2. This technique has been used in the present tests and its basis can be explained with the aid of the steady two-dimensional aerodynamic characteristics for the NACA 0012 aerofoil (the section of the *Wessex* rotor blade). The wind tunnel measurements shown in Fig. 3 are for a Mach number of 0·4 and a Reynolds number of 2×10^6 which closely represent the conditions near the tip of the Wessex blade at 270 degrees azimuth and a forward speed of 100 kn. It will be seen that at about 8 degrees incidence the lift curve becomes noticeably non-linear and simultaneously the trailing edge pressure starts to fall. This marks the onset of trailing edge-separation. As incidence increases further, the trailing-edge separation moves forward and at the same time a separation bubble forms at the foot of the leading-edge shock wave. This bubble extends further and further back as incidence increases and eventually joins up with the trailing-edge separation, producing a complete breakdown of attached flow. At this point a very large and sudden divergence of trailing-edge pressure occurs. The type of roughness used in the present flight experiments would be expected to cause the above process to occur at a lower incidence than it would with the moderate leading-edge roughness used in wind-tunnel tests for transition tripping. The extra thickening of the boundary-layer leads to an earlier formation of a separation bubble at the foot of the shock wave and an earlier onset of trailing-edge separation. This ultimately produces an earlier stall and a decrease in maximum lift coefficient.

The occurrence of trailing-edge pressure divergence is used in the present tests to indicate the onset and development of stall and its relationship with the variation in pitch link load.

5. Range of Tests

The flight programme was arranged with the object of defining boundaries of speed and normal acceleration at which a specified level of oscillatory pitch link load was reached for a particular degree and extent of roughness. Principally in order to achieve a satisfactory fatigue life of the modified pitch link, a maximum oscillatory pitch link load of $\pm 1{\cdot}56$ kN was specified by the manufacturers. However this value was well above those normally experienced at cruising speeds and allowed sufficient margin for a clear indication of rise in load due to retreating blade stall.

Preliminary tests were made without roughness added to explore flight test techniques, and pull-ups from a shallow dive were attempted with the object of obtaining a steady raised normal acceleration at constant speed for the few seconds required for recording. Some high accelerations and associated pitch link loads were recorded but the results were somewhat unpredictable and during subsequent tests turning flight was used to produce the required increased thrust loading. The results from the preliminary tests however showed certain interesting features and have been helpful in the interpretation of the main body of tests on the effects of roughness.

To help in obtaining the neccessary clearance from the manufacturer for operation with blade roughness not previously covered during type clearance flying, datum tests were made with unroughened blades outside the service flight envelope. These tests allowed a comparison to be made with the raised pitch link loads obtained outside the normal envelope during previous development flying. For the present tests, clearance was given for operation within the limits given below:

pitch link load $\pm 1{\cdot}56$ kN

$V_{max} + 10\%$, bank angle 20°

V_{max} and below, bank angle 30°

where V_{max} is the normal operating speed limit at the test weight and altitude.

The range of tests is described below:

(a) Trimmed level flight at hover and at suitable increments of speed up to the limiting pitch link load or airspeed. Tests were made with No. 60 grit and spanwise extent nil, 0·38 m, 0·76 m, 1·52 m (1·25 ft, 2·5 ft, 5 ft) inwards from the tip cap (Fig. 14).

(b) Banked turns at two fixed air speeds with a range of bank angles up to the limiting bank angle or pitch link load. The two speeds were 10 kn and 20 kn below the maximum level speed obtained in the particular test condition. These tests were carried out with smooth blades and with 1·52 m, No. 60 grit.

(c) Hovering flight at four weights from minimum to normal maximum take-off weight. These tests were made with 1·52 m, No. 60 grit: tests with unroughened blades had been made during a previous test programme.

With the exception of (c) tests were made at a take-off mass of 5700 kg and at nominally 3000 ft altitude.

6. Test Technique and Handling

For the tests in trimmed level flight a range of air speeds was chosen, starting at or near hover and increasing by 10 kn steps until the ground observer warned of a marked increase in pitch link load. Records were then made at 5 kn intervals or less until the limiting load (or speed) was reached. To obtain the trimmed speed the air speed was gradually increased with minimal control movements, gradually approaching the speed rather than overshooting it and making a correction. This technique worked well in smooth air but at speeds near and above the threshold rise in pitch link load, rapid fluctuations in the envelope of oscillatory load occurred when even slight turbulence was encountered.

In banked turns there were occasionally quite large fluctuations in pitch link load even at constant bank angle. Subsequent examination of records nevertheless showed a good correlation of pitch link load with normal acceleration ('g'), indicating the likely cause to be sideslip deviations.

There was a slight increase in the level of vibration at medium speed as the spanwise extent of the roughness was increased. The increase was most marked at the higher speeds and felt to be large with 1·5 m roughness. However vibration was not judged by the pilot to be a limitation during the present tests. The stability and control characteristics were not noticeably changed by the added roughness.

7. Results

7.1. Pitch Link Load and Trailing-Edge Pressure

Sample records of trailing-edge pressure and pitch link load with 0·76 m of roughness on each blade are shown in Fig. 4. A range of speeds is covered and at 20 kn and 40 kn the trailing-edge pressure (trace A) is relatively undisturbed with a slight once-per-revolution rise and fall due to the translational speed of the helicopter. There is a small pressure spike when the blade is on the advancing side in the region of azimuth angle $\psi = 90°$, but this tends to occur with all blade conditions and is most probably due to blade tip vortex interaction. The pitch link load (trace B) shows a basic once-per-revolution (first harmonic) variation with higher frequencies superimposed.

At 60 kn a distinct suction spike can be seen in the trailing edge pressure occurring at a blade azimuth angle just greater than 270 degrees. At the same time there is evidence of a corresponding near simultaneous upward spike in pitch link load, which because of the geometry of the linkage, corresponds to a nose-down pitching movement at the blade root. This of course would result from blade stall, the presence of which is indicated by trailing-edge pressure divergence. It should be remembered that trailing-edge pressure was monitored at one radial station only and any observed divergence of pressure does not necessarily mean

the onset of blade stall generally (it might have occurred already elsewhere on the blade). Again the blade response plays its part in transmitting loads to the root. Thus it is not necessarily to be expected that the peaks in trailing-edge pressure will be coincident with those of load. By 87 kn two distinct suction spikes are present with corresponding spikes in pitch link load. At 93 kn the pressure spikes have almost merged and persist throughout the fourth quadrant in azimuth. By this time the pitch link load has reached the set limit of $\pm 1{\cdot}56$ kN and in this regime taken the appearance of a divergent oscillation superimposed on the basic first harmonic variation.

A similar time history during five successive revolutions of the rotor is given in Fig. 5. It was obtained with 1·52 m roughness and at a speed of 75 kn: the highest reached in this particular condition. The large-amplitude high-frequency content of the pitch link load is particularly marked and again shows a rough correspondence of pressure spikes with the largest of the loading peaks in the fourth quadrant of azimuth. These time histories are analysed and discussed in greater detail later in Section 8.2.

At speeds below 20 kn corresponding changes in trailing edge pressure and pitch link load again occur becoming most pronounced during hovering flight. The local C_L is high in the tip region during hovering flight due to the interaction with the tip vortices trailed from preceding blades[3]. In near-hovering flight the small translational velocities cause this interaction to produce large and rapid fluctuations of load at radial positions near the blade tip. The results indicate that leading-edge roughness leads to premature blade stall in this regime of flight, in addition to that at the higher speeds.

7.2. The Effect of Roughness on Speed and Thrust Limitations

A broad picture of the results has been obtained by using the amplitude of the trailing-edge pressure divergence and overall amplitude of the oscillatory pitch link load as indicators of the effect of leading-edge roughness (typical values are shown arrowed in Fig. 4). Figs. 6 to 9 show these quantities plotted against speed for unroughened blades, and with 0·38 m, 0·76 m and 1·52 m roughened respectively in level flight. Oscillatory pitch link load shows a well defined pattern with speed. Once out of the low speed regime, the load reduces to about 0·9 kN in all cases, where it remains constant until a sharp rise occurs at some critical speed. This occurs earlier for each increase in roughness until, with 1·52 m roughened, the maximum allowable load of $\pm 1{\cdot}56$ kN is reached at approximately 70 kn compared to an estimated 115 kn unroughened. The trailing edge pressure excursions follow a similar pattern and indicate the strong correlation between retreating blade stall and oscillatory pitch link load.

The scatter at air speeds greater than 60 kn with 1·52 m of roughened blade (Fig. 9) is an indication of high sensitivity to small changes in thrust resulting from minor control movements and slight turbulence in this condition.

At low speeds there is a general rise in oscillatory pitch link load and corresponding increase in trailing-edge pressure divergence with the exception of unroughened blades. In this particular case there is a slight fall in pitch link load accompanied by only a small increase in trailing-edge pressure divergence. Examination of the actual records shows there are two pressure spikes per revolution with approximately 180 degrees spacing, and this double pressure signature differs from the single signature obtained with roughened blades. The double signature might be explained by blade vortex interactions but the lack of a corresponding rise in pitch link load remains an anomaly.

Results obtained during steady turns are given for unroughened blades (Fig. 10) and for blades with 1·52 m roughness (Fig. 11). Again, the same general correlation of pitch link load with trailing-edge pressure divergence is evident; both quantities increasing with normal acceleration for a particular speed and blade condition. As expected, the rate of increase with normal acceleration is greatest at the higher speed for each blade condition, except for the early steep rise in trailing-edge pressure divergence with roughened blades (Fig. 11).

The results obtained have been used to construct a Speed-Normal Acceleration ($V-g$) boundary for the limiting oscillatory pitch link load of $\pm 1{\cdot}56$ kN (Fig. 12). It will be seen that in level flight with 1·52 m roughness the speed is reduced from 117 kn to 72 kn; the effects of intermediate roughness being approximately proportional to extent. Normal acceleration reduces the limiting speed by approximately 10 kn per 0·1 g.

7.3. The Effect of Roughness on Power Required

The effect of extent of roughness on rotor torque (and power since rotor speed was nominally constant) is shown in Fig. 13. The results have been non-dimensionalised to reduce the consequence of small differences in test conditions. At low speeds (low values of tip speed ratio, μ) there is no particular trend in the torque

required with extent of roughness, but as speed increases there is evidence, despite the scatter, of an early rise in torque dependent on the extent of roughness. The trends shown are in agreement with the onset and progression of retreating blade stall evident in Figs. 6 to 9, and reflect the large increase in profile drag of the blades due to premature stall of the roughened blades.

8. Disucssion

8.1. Onset of Blade Stall

Although the total amplitude of oscillatory pitch link load is very useful as a broad indication of load variation a more detailed analysis is helpful in the interpretation and appreciation of events. Thus, in Fig. 14 further details of load variation and trailing-edge pressure are tabulated together with corresponding diagrams of the extent of roughness and relative position of the pressure transducer. Here some judgment has been used in deciding the values of speed at which the characteristic changes occur, since there is scatter in the results, but they are considered an accurate indication of trends excluding the near-hovering flight regime.

The first column gives the speed at which the initial change in character of the pitch link load occurs. This change has been mentioned in Section 7.1 and is for example evident in Fig. 4, where between 60 kn and 80 kn a pronounced upward spike (nose down pitching moment) can be seen. As the roughness increases in extent, the speed at which the change in character of the pitch link load occurs progressively decreases. These speeds are identical with those at which trailing edge pressure divergence first occurs (final column) except for 0·38 m roughness when the pressure transducer is not directly behind the roughened portion and intermittent divergence occurs at a higher speed. It is clear therefore that the change in load characteristics is directly associated with the onset of blade stall.

Insight into the effect of the spanwise extent of roughness on forward speed limitation from blade stall can be gained by examining the distribution of lift coefficient in the tip region of the retreating blade. Fig. 15 shows the radial distribution of C_L on the retreating blade obtained from NASA flight tests of the *S58* helicopter[4] (basically similar to the *Wessex*) with normal blade finish at 78 and 108 kn. The 1·52 m limit of roughness has been superimposed and it will be seen that the highest values of C_L occur at the inboard edge of the roughened area with C_L reducing towards the blade tip. The degree of premature stall would therefore tend to increase as the extent of roughness increases inwards from the tip and would only be relieved by a reduction in speed and consequent lowering of the general level of C_L values in this region of the rotor disc. This interpretation explains the progressive reduction in speed at which the change in the character of the pitch link load (indicative of stall) first occurs as the extent of roughness increases.

An attempt has been made to estimate the reduction of maximum C_L due to roughness. This has been done by estimating the value of C_L at the spanwise speed and azimuth angle ($\psi = 270°$ approx.) at which pressure divergence occurs. On the basis that $C_{L_{max}}$ has been achieved at the stage at which trailing edge pressure divergence occurs, this calculated value of C_L is the value of $C_{L_{max}}$. Now as the forward speed reduces, the value of C_L reduces on the retreating blade and the fact that trailing edge pressure divergence occurs at a lower value of forward speed for the roughened blades is the evidence that roughness has reduced the blade $C_{L_{max}}$. The difference in calculated C_L for the two speeds at which trailing edge pressure occurs is then taken to be the difference in $C_{L_{max}}$ for clean and roughened blades.

Although measured values of rotor disc incidence taken from previous flight tests were used in the estimation, the method for calculating C_L was a crude one, using the simplifying assumption of uniform induced velocity. Such simplification can be defended on the grounds that differences in C_L rather than absolute values are being estimated. Also the estimation of $C_{L_{max}}$ reduction in this way, assumes that any unsteady aerodynamic stall delay is small or at least constant at the two speeds. For these reasons the estimate though useful, should be considered a guide only.

The pressure transducer is directly behind the inner portion of the roughened leading edge with 0·76 m roughness band (Fig. 14), and initial trailing edge pressure divergence occurs at 70 kn. The difference in calculated C_L between this condition and the corresponding condition at 105 kn with unroughened blades gives $\Delta C_L = 0·21$. It could be argued that the still lower pressure divergence speed associated with the roughness band of 1·52 m might be used giving a greater ΔC_L value. However this could be misleading as the earlier indication of stall at the transducer that obtains for the larger roughness band will be partly due to straightforward re-distribution of loading on the blade caused by cyclic pitch change necessary to re-trim the rotor with the extended stall area; also the three-dimensional growth of the stalled area and changes in the pattern of trailing vorticity must also play a part in determining the local loading changes accompanying any

change in the length of the roughness itself. Alternatively the speed difference between unroughened blades and blades with the 0·38 m roughness band might be used with the change in character of the pitch link load as an indicator of stall, giving a smaller reduction of $C_{L_{max}}$ due to roughness. However, the proximity of the roughness band to the tip may affect the comparison in this case and also the indication is less direct that that of trailing edge pressure divergence. For the reasons given a reduction of $C_{L_{max}}$ of 0.2, i.e. some 20 per cent of the unroughened value, is considered to be the best estimate of the effect of roughness.

The reliability of this estimate is enhanced by inspection of blade loading distributions recently measured on the same aircraft[5] during other work (Fig. 16). Although the blades were slightly modified in planform at the tip, the speed change described previously results in a change of C_L of the same order when maximum values in the region of $\psi = 270°$ are compared.

Although no checks have been made on the possible loss in $C_{L_{max}}$ in two-dimensional conditions with the degree of roughness used in the present flight experiments, wind tunnel tests have been made on a NACA 0012 aerofoil with a leading edge roughness band for transition fixing. In this case, roughness produced a 10 per cent loss of $C_{L_{max}}$ at $M = 0{\cdot}35$ (the appropriate flight local retreating blade Mach number) and Reynolds number close to the flight value. The roughness was of course much less comparatively than used in the flight experiment (2·5 times less relative to respective chords).

Overall, the results clearly indicate the importance of minimising leading edge roughness from whatever cause in order that the full potential of the helicopter is realised and that limiting loads and performance are not reached prematurely. The results also highlight by implication the sensitivity and importance of appropriate scale roughness in the prediction of full scale results from model rotor tests particularly at the limits of performance when retreating blade stall is present.

8.2. Blade Torsional Oscillation

With all blade conditions a pronounced oscillation in pitch link load occurs at the higher speeds and increases in amplitude as speed increases further. It develops from the initial spike in load referred to previously and some 2–3 oscillations are usually present. At the limiting speeds the oscillation develops towards the end of the third quadrant of azimuth, is roughly constant or slightly divergent through the fourth and rapidly damps to near zero in the beginning of the first quadrant. The earliest speed at which a pronounced oscillation is visible for the various extents of roughness is recorded in Fig. 14, second column.

The high frequency oscillation of pitch link load is particularly noticeable with 1·52 m roughness at the highest speed tested (Fig. 5). In this condition it persists to some degree throughout the complete range of azimuth. Again there is a rapid increase in amplitude during the third quadrant, continued divergence during the fourth and rapid damping to a relatively low amplitude in the beginning of the first quadrant.

Harmonic analysis of results with 1·52 m roughness are given in Fig. 17 for speeds of 40 and 75 kn. The amplitudes of each harmonic up to the eleventh are shown normalised with respect to the first harmonic amplitude at 40 kn. The harmonics of all but the first are small at 40 kn, but at 75 kn, the sixth is large and dominant reflecting the large contribution of the high frequency oscillation when blade stall is present.

The larger amplitudes in load are accompanied by corresponding spikes of trailing-edge pressure divergence. On the hypothesis of a stall flutter type of oscillation these would reflect blade loading changes primarily as a result of incidence changes due to torsional oscillation of the blade itself rather than direct changes in incidence inherent in the rotor wake velocity distribution. Also during oscillation in and out of stall, the blade would be expected to be stalled in the region of maximum nose-up deflection. No torsional strain gauges were fitted to the blades so no direct confirmation of blade twist was obtained. However the pitch link load is proportional to the torsional strain at the blade root and maximum nose-up incidence at the tip will occur at points such as those marked 'A' and 'B' in Fig. 5 if the first torsional mode of the blade is the principal mode excited. This is because the pitch link is attached to the blade pitch change horn which is forward of the quarter chord and is in maximum tension when the blade is at maximum positive incidence.

The importance of the first mode torsional response of the blade in determining control loads was shown in the extensive analysis of flight data obtained from *NH-3A* and *CH-53A* helicopters[6]. Results showed the torsional response of the blade in the first mode to be a major factor in the build up of large fluctuating control loads in the fourth quadrant of azimuth. The contribution from coupling due to blade bending in flap and lag was relatively small. The conclusions reached were that although stall flutter was likely to be the dominant factor in conditions of deep blade stall, in the less severe conditions analysed, there was little direct correlation between aerodynamic moment (obtained from blade pressure distribution) and pitch link load, and that the load was largely the result of the forced torsional response of the blade to the time varying aerodynamic moment.

In contrast the results with roughened blades described here show a noticeably direct correlation between the degree of stall and the larger oscillatory pitch link loads, but the phasing requires comment. If it is assumed that points A and B in Fig. 5 represent maximum nose-up deflection at the blade tip then the trailing-edge pressure divergence lags the motion to such an extent that flow reattachment is delayed until well after maximum nose-down displacement. This is particularly true of excursion A. Excursion B would represent a more expected phasing if, as is usually the case, trailing-edge pressure divergence results in a nose-down aerodynamic pitching moment. This moment would then reinforce the nose-down torsional swing of the blade producing negative damping consistent with a divergent oscillation of the blade. It should be remembered that changes in incidence inherent in the induced velocities in the rotor wake are also superimposed on those due to oscillation of the blade itself and will affect the phasing between control load and trailing-edge pressure peaks. Any such effects would be large and rapid if attributable to the close proximity of the blade with vortices trailing from the tips of preceding blades. The possible blade/vortex crossing positions in the plan view sense, assuming a simple cycloidal wake model, are shown in the centre revolution in Fig. 5. Only the first intersections with the preceding three blades are included. No obvious correlation with trailing-edge pressure divergence or load is apparent and any incidence changes present are not directly attributable to this cause.

On the other hand a fairly large perturbation in C_L does occur at and beyond $\psi = 270°$ as seen from the flight test results[5] in Fig. 16. This is not attributable to stall since the values of C_L are relatively low but is due to the less localised and integrated effect of vortices embedded in the wake. The two peaks in C_L correspond fairly well with excursions in pressure and load in the present tests (Fig. 5) and would tend to produce an underlying forcing of the stall and load oscillations with roughened blades. In all cases however, the second amplitude of trailing-edge pressure and load excursion is greater than the first as seen for example in Figs. 4 and 5 whereas the second peak in C_L (Fig. 16) is lower. This would imply that the torsional damping is small but not necessarily negative as required during divergent stall flutter oscillations. Indeed it should be remembered that although the second value of C_L is lower than the first the chordwise velocity and Mach number will be greater due to the change in azimuth so that the load may possibly be higher. Again the value of $C_{L_{max}}$ will also be lower at the higher M. Nevertheless the phasing of the trailing edge pressure divergence and load is consistent with a stall flutter type of oscillation at least in the final stages. Additional evidence discussed below, that the oscillation occurs at the frequency of the first torsional mode of the blade, adds further support to this view.

Several static ground tests were made on the stiffness of the blade and control system to aid determination of the effective torsional frequency of the first mode of free vibration. Torsional loads were applied at the blade tip, and torsional deflections at the tip, pitch horn and any carry-over to the three other blades measured. The tests were made with the blades at various positions relative to the three jacks which control the swash plate position. The results showed that some 20 per cent of the torsional deflection of the tip occurred in the control system. Also the effective stiffness at the tip varied by about 10 per cent dependent on blade azimuth position and up to 5 per cent of the tip's torsional deflection carried over the swash plate causing change in pitch of the opposite blade. Calculation shows a control system flexibility of 20 per cent reduces the basic first mode torsional frequency of the blade alone from $7{\cdot}3\Omega$ to 6Ω.

The oscillatory pitch link loads measured in flight therefore occur at the first mode torsional frequency as other investigations (e.g. Ref. 5) have reported. There is no apparent change in frequency even during the largest torsional oscillations (Fig. 5) and this implies the effective aerodynamic stiffness component is relatively small. The tip deflection for a given root moment when vibrating *in vacuo* may not therefore be too unrepresentative of actual conditions. Estimates show a tip torsional deflection of approximately ± 2 degrees for the prescribed pitch link load limit of 1·56 kN.

The magnitude of the trailing edge pressure divergence generally is relatively large, for example, at the condition shown in Fig. 5 the values are of the order of 10 kN/m^2, corresponding to an incremental pressure coefficient of $-0{\cdot}7$ based on the local dynamic head at the appropriate azimuth angle. They are therefore of the order 1·5 times greater than the total variation of trailing edge C_p over the range tested statically (Fig. 3). It is possible that vorticity from time and spanwise loading changes are contributory factors.

As mentioned previously the oscillations in control load persist to some degree throughout the complete range of azimuth. Feed back between opposing blades through the flexibility of the control system is a contributory factor, but the static measurements described above indicate a coupling factor of less than 5 per cent. Ref. 6 suggests the relatively rapid changes in pitching moment on the advancing blades appear to excite blade torsional oscillations that persist and serve as initial conditions for retreating blade response. What is very noticeable in the present results is the extremely rapid damping of the control load oscillation in the regime of zero azimuth angle. The mechanism responsible requires further investigation.

8.3. Pull-up Manoeuvres

As mentioned in Section 5 some preliminary tests with unroughened blades in pull-up manoeuvres were made at the start of the present test programme. These will now be described briefly to demonstrate the difference in type of loading action from that measured in level flight with roughened blades in the context of the previous discussion. In this type of maneouvre and in turns where the increased thrust increases vortex strength, and positive rate of pitch makes blade vortex intersection more likely (i.e. decreases the vertical separation) related increases in control loads may occur[7]. A sample time history of pressure divergence and pitch link load is given in Fig. 18. It will be seen that 1·7 seconds after the start of the manoeuvre three large spikes of trailing edge pressure divergence occur in the fourth quadrant of azimuth. The position of possible blade vortex intersections has been added for time 1·7 and 2·6 seconds. In each case there is a general correspondence in the fourth quadrant but with some shift in phasing which could be due to wake distortion. This must occur to some degree in practice and is not included in the simple model. However there is no obvious correlation between pressure divergence and peaks of pitch link load which are of a higher frequency than with roughened blades in level flight. The dominant feature is a very large first harmonic load content. After 4 seconds this position of the blade is stalled for one third of a revolution with extremely high oscillatory loads. Due to the relatively short life of the modified pitch link in these conditions of high loading, this type of manoeuvre was subsequently curtailed during the present test programme. This characteristic behaviour of blade vortex intersection is not evident in the level flight tests of roughness and reinforces the previous conclusion that blade vortex intersection is not considered to be a significant factor in the increase in control load measured.

9. Conclusions

Flight tests have been made on a *Wessex* helicopter with blades artificially roughened to simulate the effects of erosion which may become severe on rotor blades with unprotected light-alloy leading edges in prolonged operations in rain or sea spray. Most helicopters including the type tested, are normally flown with a protective leading-edge strip or the leading edge is fabricated from stainless steel which is much less susceptible to rain erosion.

Tests have been made to determine the effect on blade torsional loads (oscillatory pitch link load) and performance with a degree of roughness equivalent to light to moderate erosion of unprotected light-alloy blades. A deterioration at the leading edge eventually occurs in some degree even with protected blades and the results should be useful in this general context.

Trailing-edge pressure divergence has also been used as a 'stall indicator' during tests in which the spanwise extent of roughness in the tip regions was varied. This provided insight into the effects of leading-edge roughness on stall and corresponding increase in blade oscillatory torsional loads. The principal findings are summarised below:

(1) The speed at which a designated limiting oscillatory pitch link load was reached reduced from 117 kn to 73 kn with a roughness band of 1·52 m extending inwards from the blade tip. Corresponding speeds for roughness bands of 0·76 m and 0·38 m were 93 kn and 105 kn respectively.

(2) Actual erosion reduces in severity inwards from the tip and a roughness band of 0·76 m, and the associated limiting speed of 93 kn are thought to best represent the extent and limiting speed for light to moderate erosion in practice. This relatively small degree and extent of roughness therefore caused the marked reduction in limiting speed of 24 kn.

(3) Roughness reduces appreciably the thrust available for the designated oscillatory limit of pitch link load.

(4) The effect of roughness on power required has been measured and shows a premature rise in power with speed dependent on the extent of roughness.

(5) There is a close correlation between blade stall as indicated by trailing-edge pressure divergence and the change in character and increase in amplitude of oscillatory pitch link load.

(6) There is evidence that the large oscillatory control loads of the retreating blade are accentuated by stall flutter occurring at the frequency of the first torsional mode. The effect of roughness is to reduce the speed at which this occurs.

(7) The results suggest a reduction of maximum lift coefficient, $\Delta C_L \simeq 0{\cdot}2$ due to the degree of roughness tested but this value must be treated with reservation.

(8) The results by implication emphasise the sensitivity and importance of appropriate scale roughness in predicting full scale performance from model tests particularly in those conditions when retreating blade stall is present. Finally the results provide some feel for the separate but in some respects similar topic of rotor blade icing.

SYMBOLS

c	Blade chord
C_L	Lift coefficient
C_p	Pressure coefficient based on dynamic pressure
g	Acceleration due to gravity
M	Mach number
q_c	Torque coefficient $Q/\pi\rho s\Omega^2 R^5$
Q	Rotor torque
R	Rotor tip radius
Re	Reynolds number
s	Rotor solidity
t_c	Thrust coefficient = $T/\pi\rho s\Omega^2 R^4$
T	Rotor thrust
V	Indicated airspeed
x	Chordwise distance from leading edge
α	Incidence
μ	Rotor tip speed ratio
ρ	Air density
ψ	Blade azimuth
Ω	Rotor rotational speed

REFERENCES

No.	*Author(s)*	*Title, etc.*
1	A. W. Moore, N. C. Lambourne and L. Woodgate	Comparison between dynamic stability boundaries for NPL 9615 and NACA 0012 aerofoils pitching about the quarter-chord. A.R.C. C.P.1279 (1974)
2	H. H. Pearcey	A method for the prediction of the onset of buffeting and other separation effects from wind tunnel tests on rigid models. A.G.A.R.D. Report 223 (1958)
3	M. J. Riley and P. Brotherhood ..	Comparative performance measurements of two helicopter profiles in hovering flight. R.A.E. Technical Report 74008 (1974)
4	J. Scheiman	A tabulation of helicopter rotor blade differential pressures, stresses and motions as measured in flight. NASA TM X-952 (1964)
5	P. Brotherhood	Some aerodynamic measurements in helicopter flight research. *The Aeronautical Journal*, Royal Aeronautical Society Vol. 79, pp 450–465 (1975)
6	E. A. Beno	Analysis of helicopter manoeuvre—loads and rotor-loads flight test data. NASA CR-2225
7	J. F. Ward	Helicopter rotor periodic differential pressures and structural response measured in transient and steady manoeuvres. Pre-print 423 American Helicopter Society (1970) Also *J. Am. Hel. Soc.*, Vol. 16, pp 16–25 (1971)

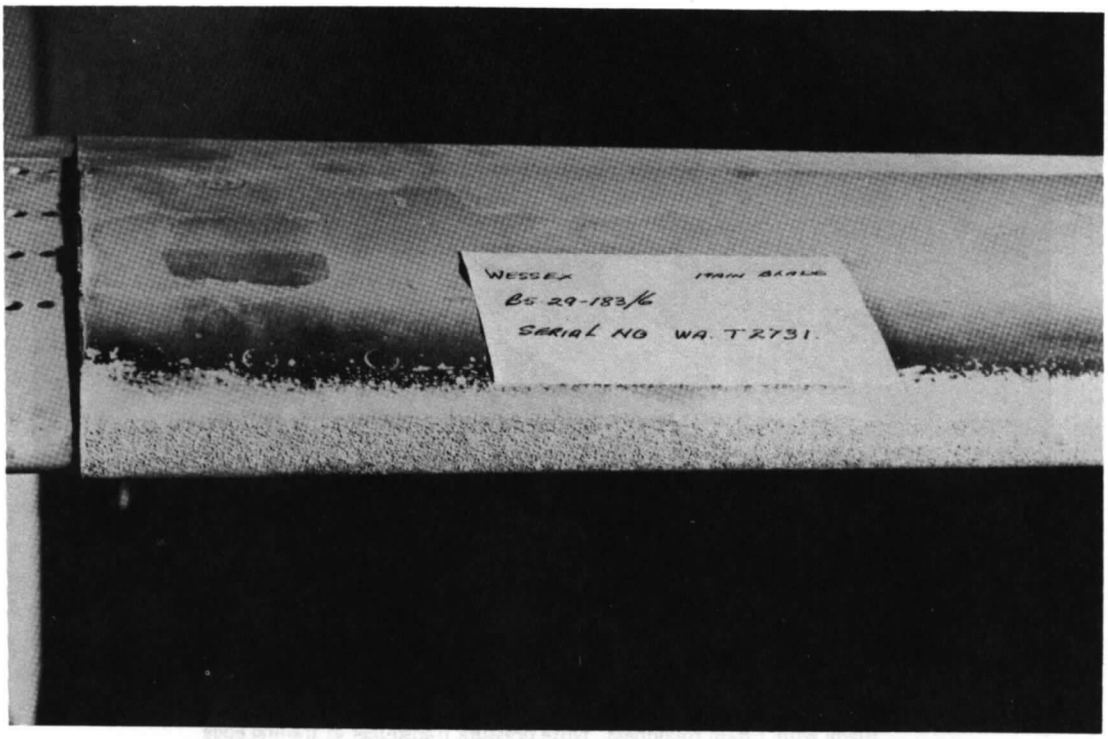

Heavy erosion of Wessex main blade (tip cap removed)

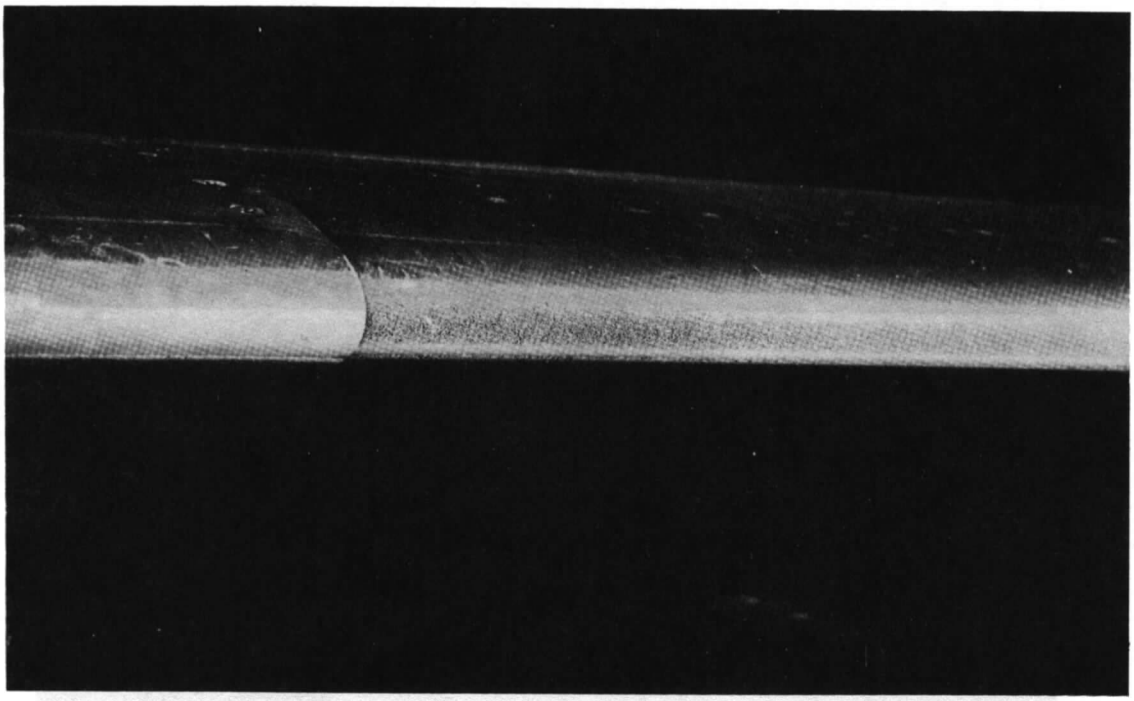

Moderate to heavy erosion of Sea King main blade

FIG. 1. Erosion of unprotected light alloy rotor blades. The level of erosion depicted would be unacceptable without remedial action. Normally these blades are protected with a renewable polyurethane strip, the surface of which usually erodes at a very low rate.

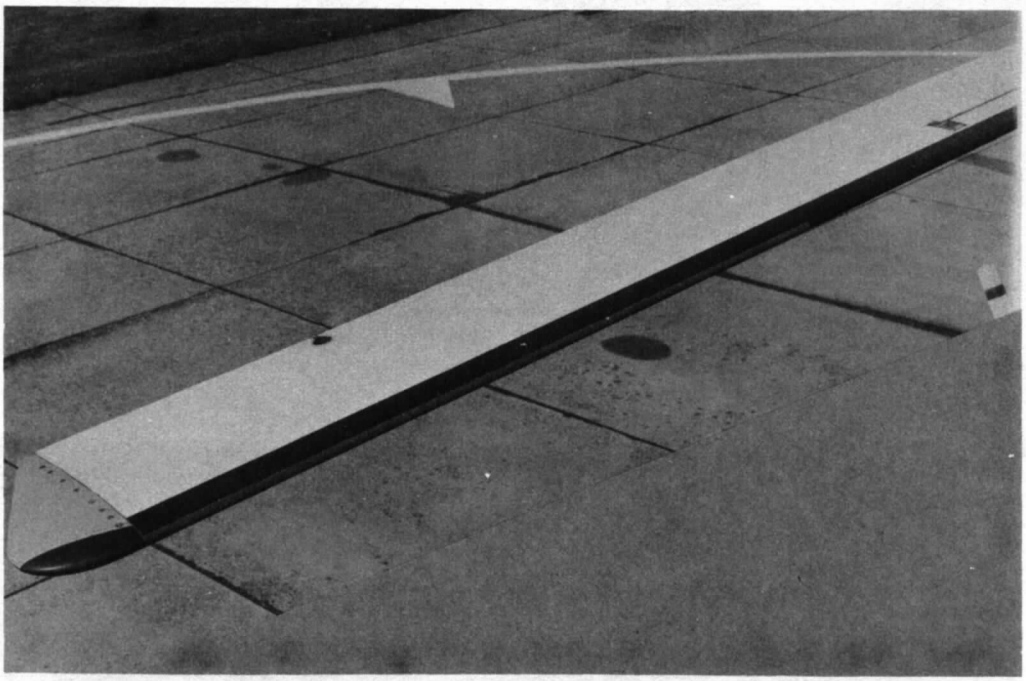

Blade with 1.52m roughness. Note pressure transducer at trailing edge

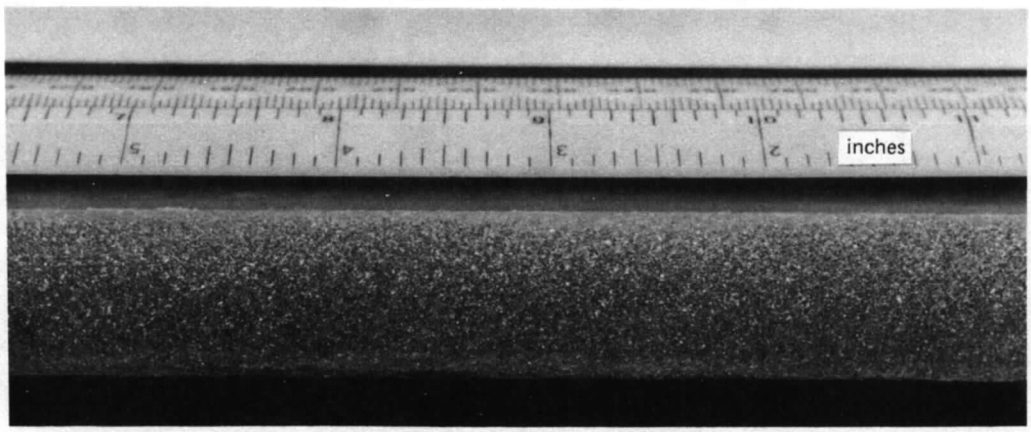

Degree of roughness at start of tests

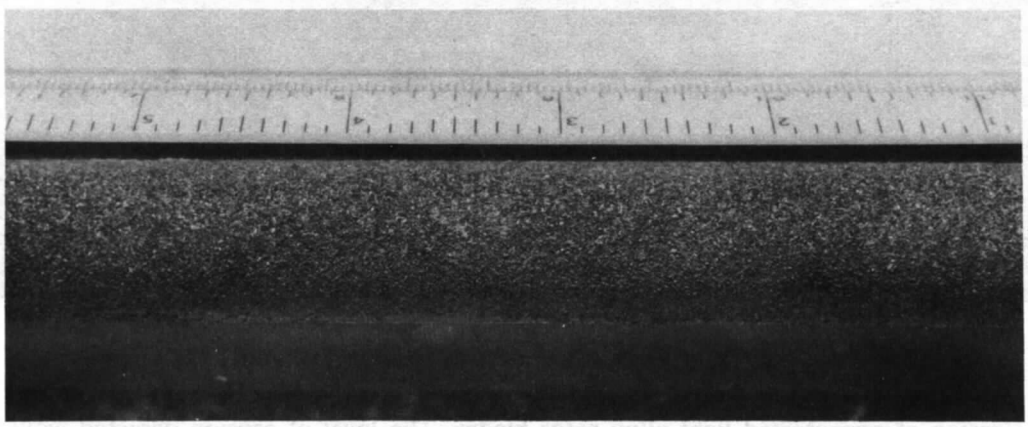

Degree of roughness at end of tests

FIG. 2. Simulated erosion on *Wessex* blade.

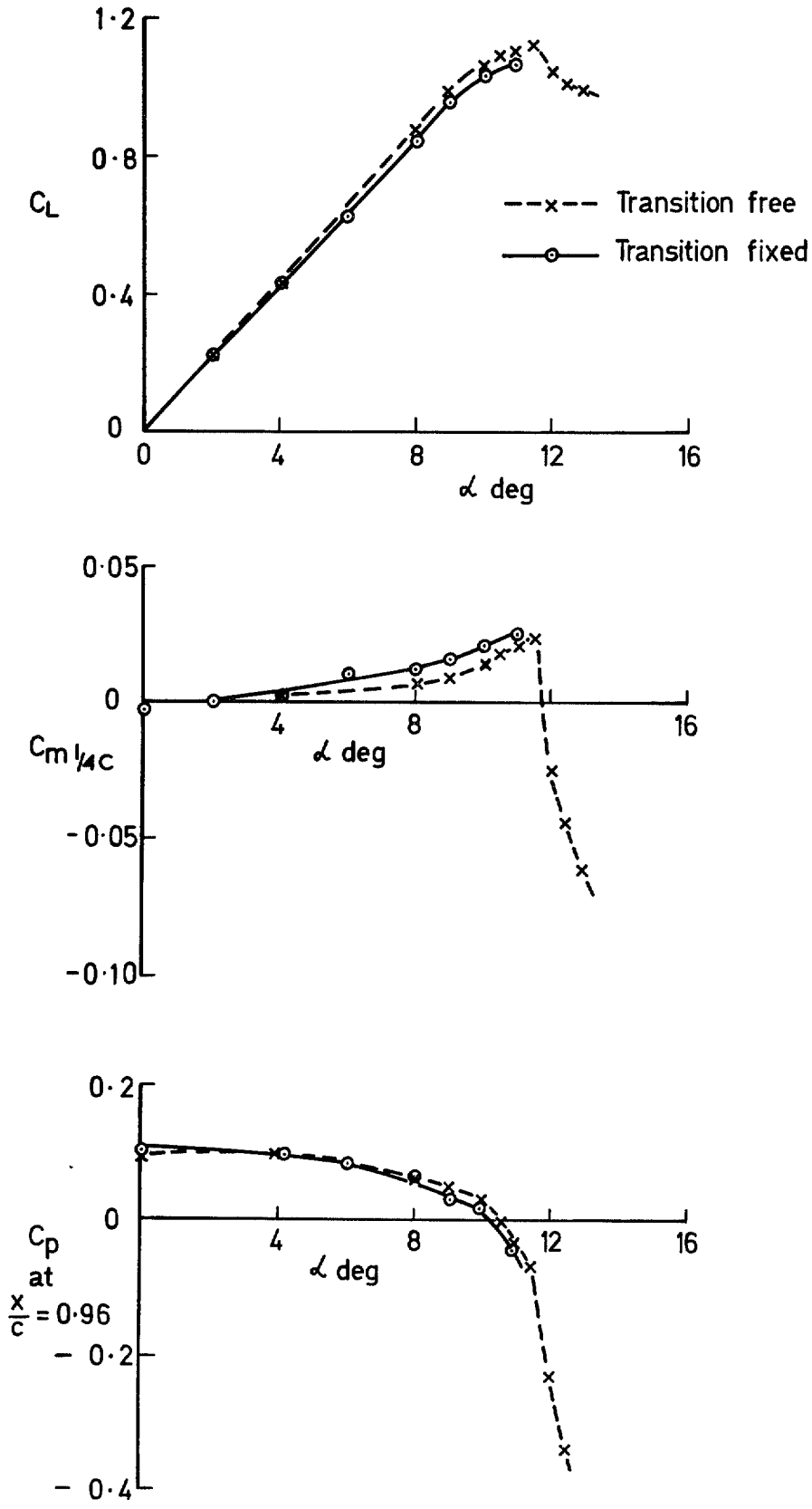

FIG. 3. Steady 2D wind tunnel results of lift, pitching moment and trailing-edge pressure divergence coefficients. NACA 0012 section, $M = 0{\cdot}4$, $Re = 2 \times 10^6$.

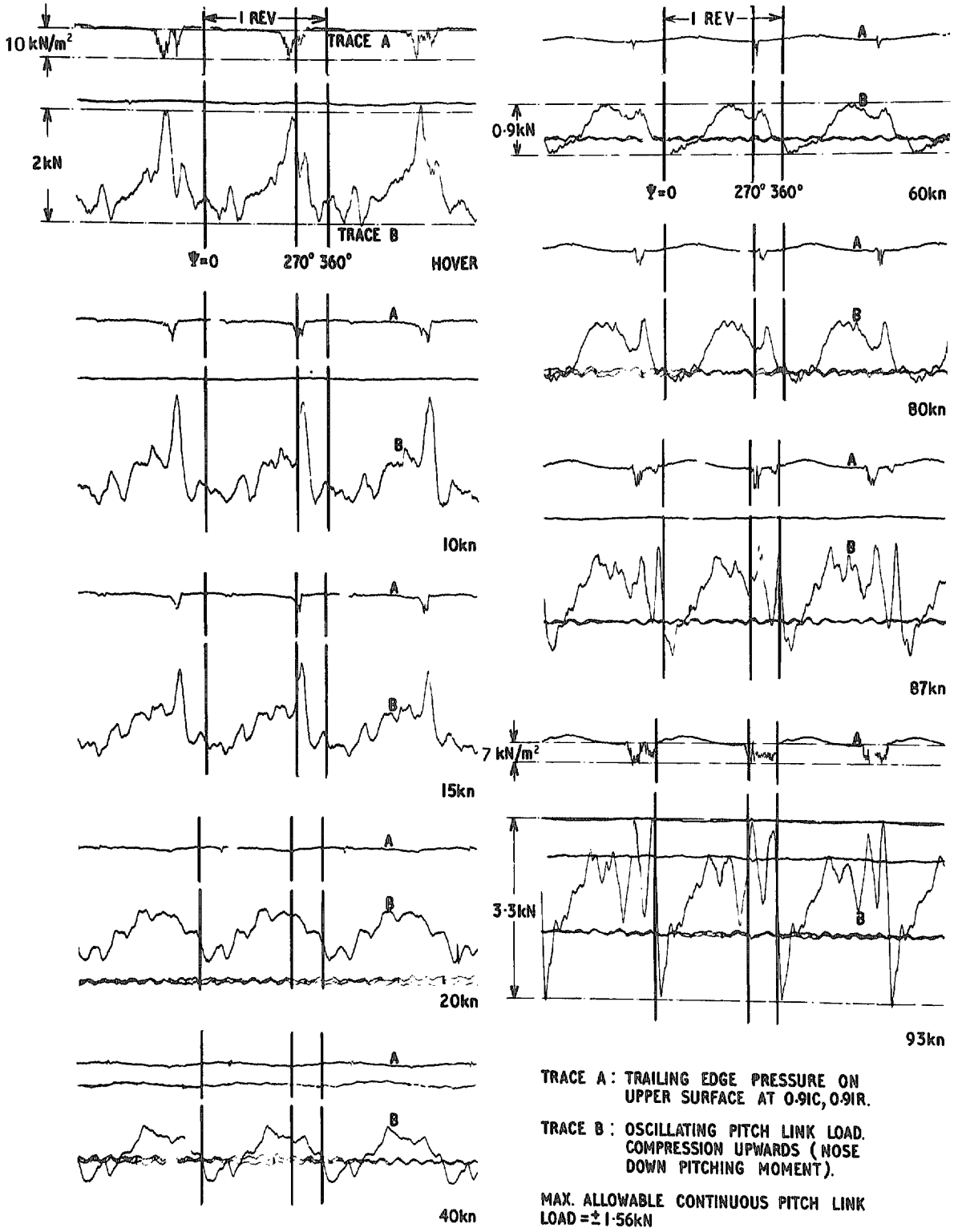

FIG. 4. Photographic traces of trailing-edge pressure, and pitch link load in level flight. Outer 0·76 m of leading edge roughened.

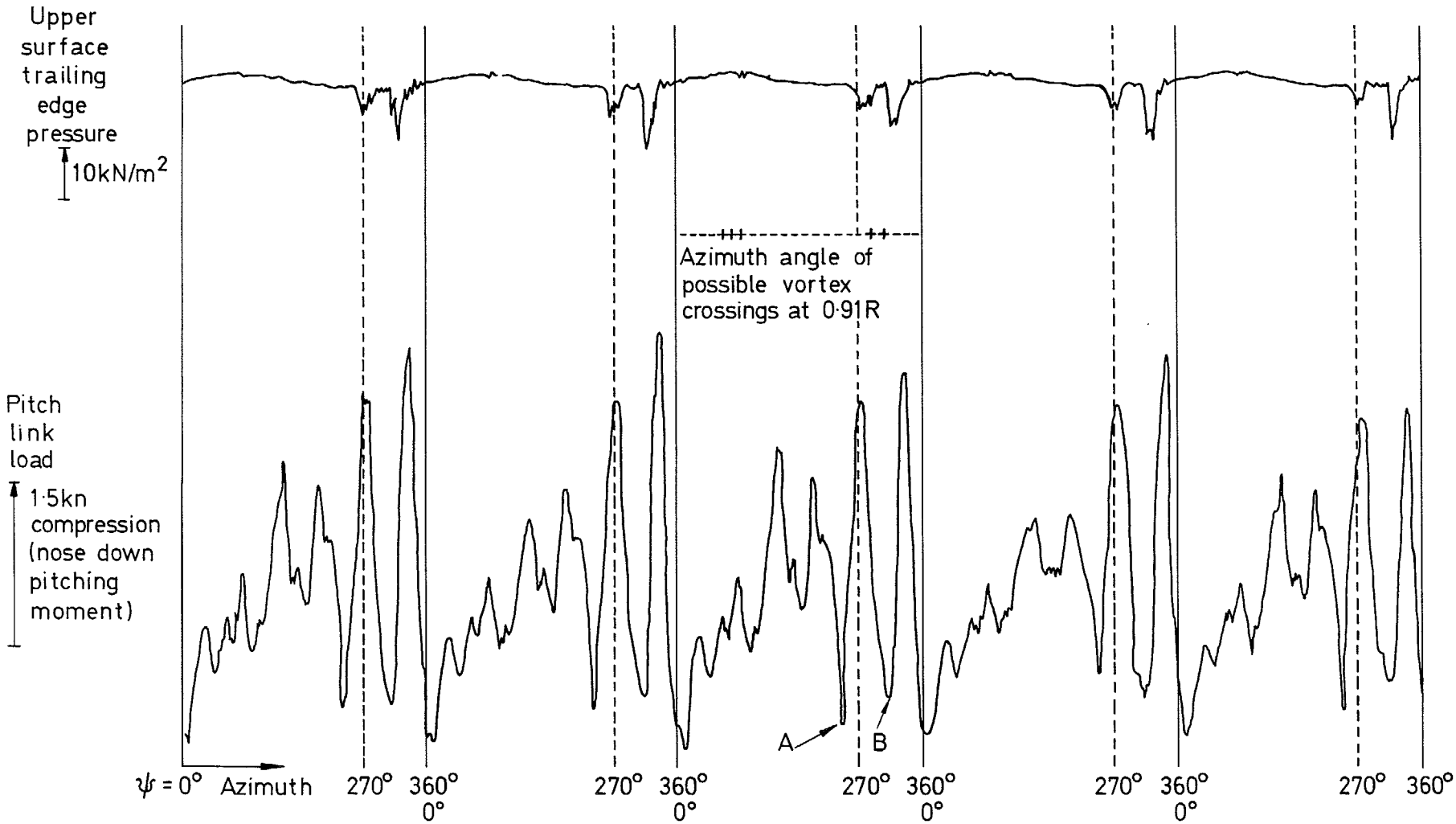

FIG. 5. Five successive revolutions of trailing-edge pressure and pitch link load. Speed 75 kn, 1·52 m roughened.

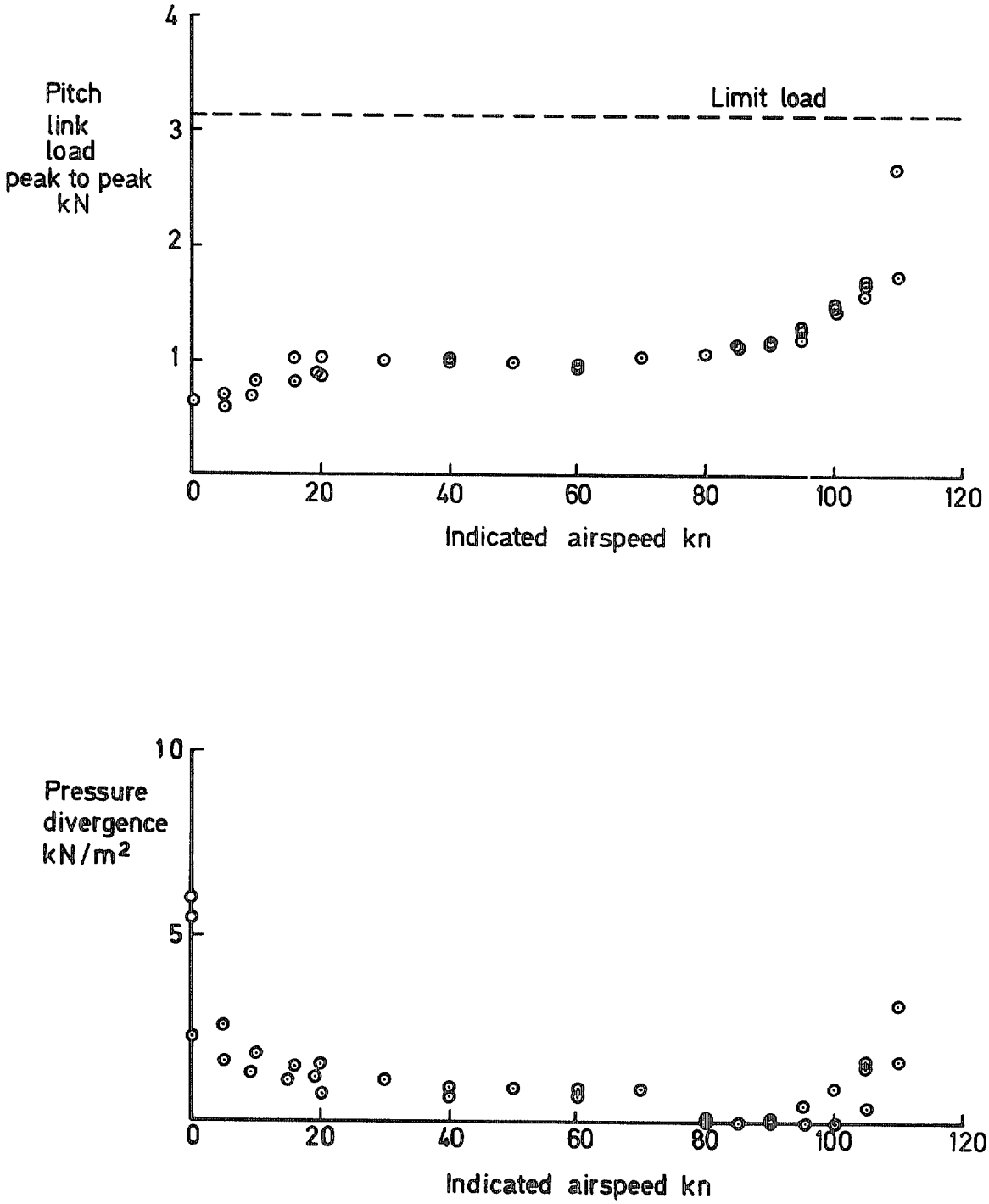

FIG. 6. Variation of oscillatory pitch link load and TE pressure divergence with speed in level flight. Unroughened blades.

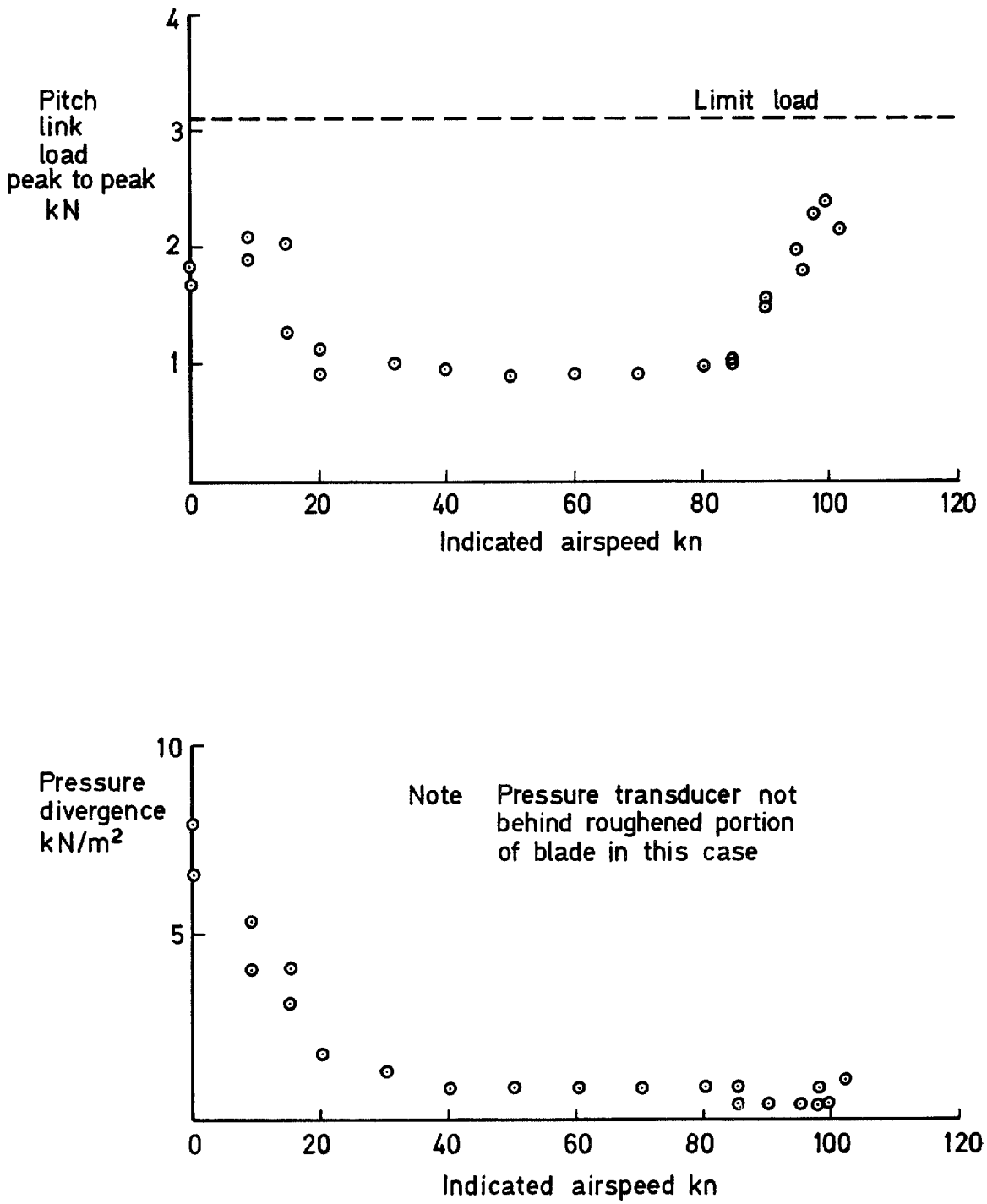

FIG. 7. Variation of oscillatory pitch link load and TE pressure divergence with speed in level flight. Outer 0·38 m roughened.

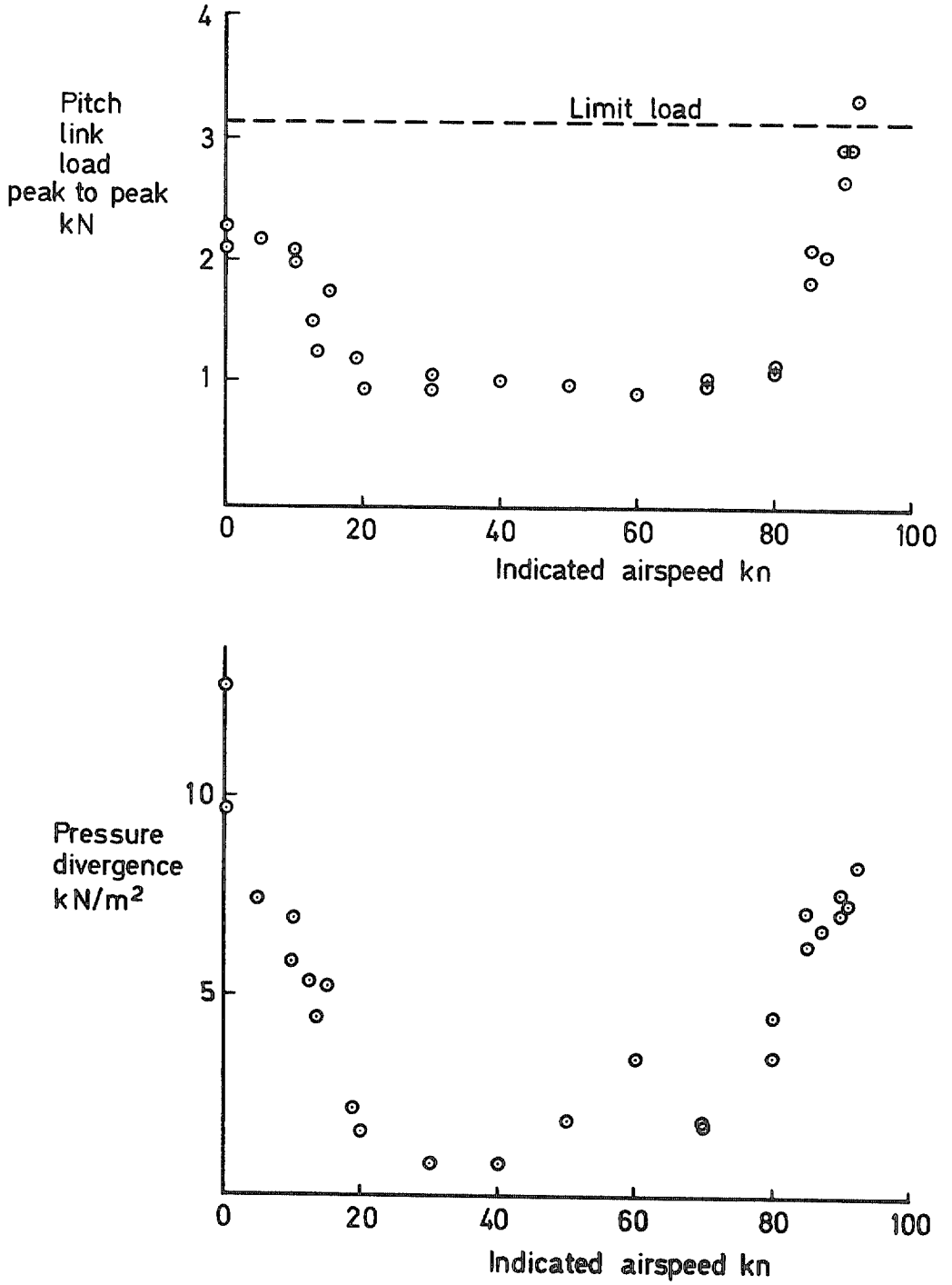

FIG. 8. Variation of oscillatory pitch link load and TE pressure divergence with speed in level flight. Outer 0·76 m roughened.

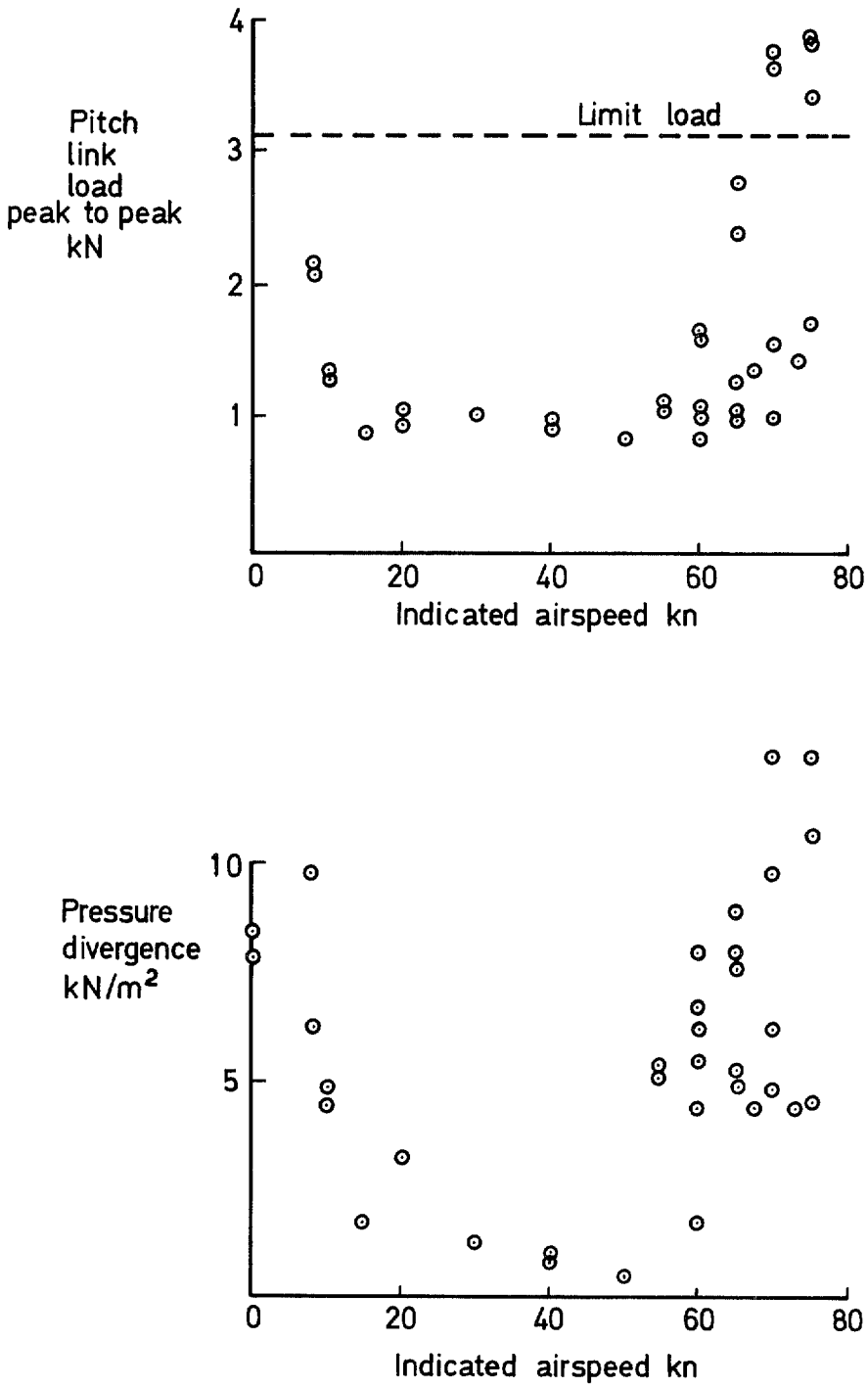

FIG. 9. Variation of oscillatory pitch link load and TE pressure divergence with speed in level flight. Outer 1·52 m roughened.

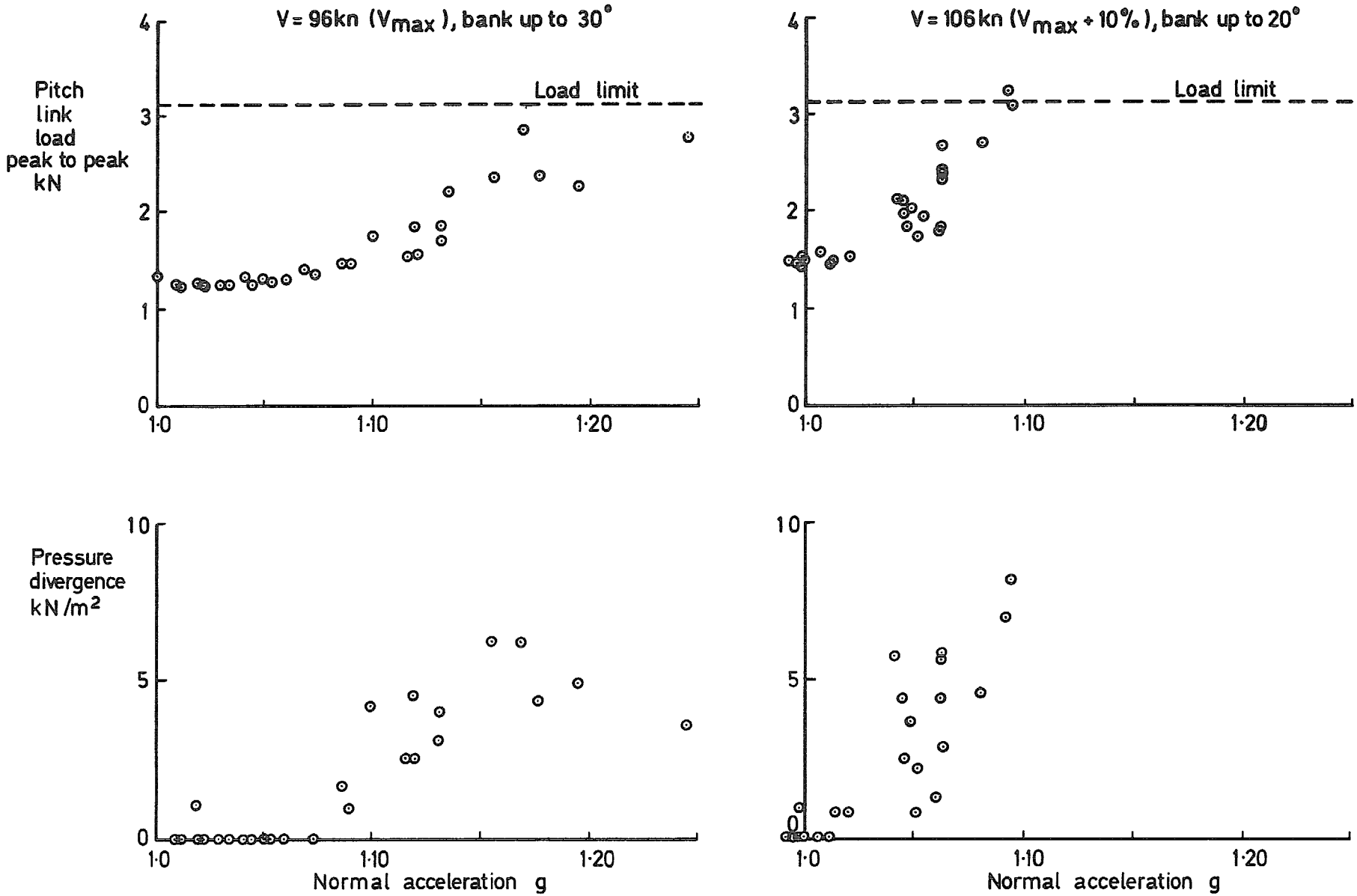

FIG. 10. Variation of oscillatory pitch link load and TE pressure divergence with 'g' during turns. Unroughened blades.

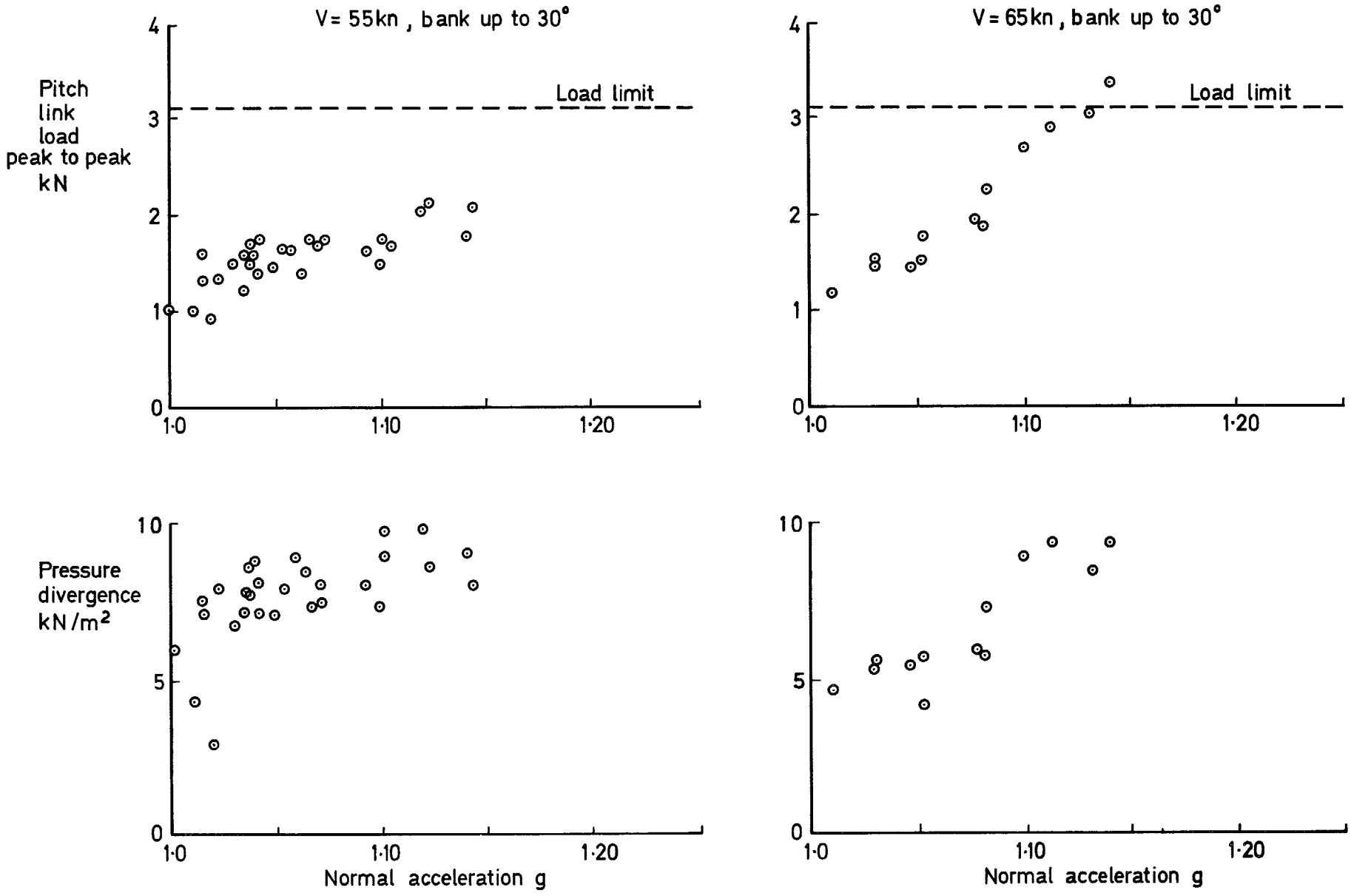

FIG. 11. Variation of oscillatory pitch link load and TE pressure divergence with 'g' during turns. Outer 1·52 m roughened.

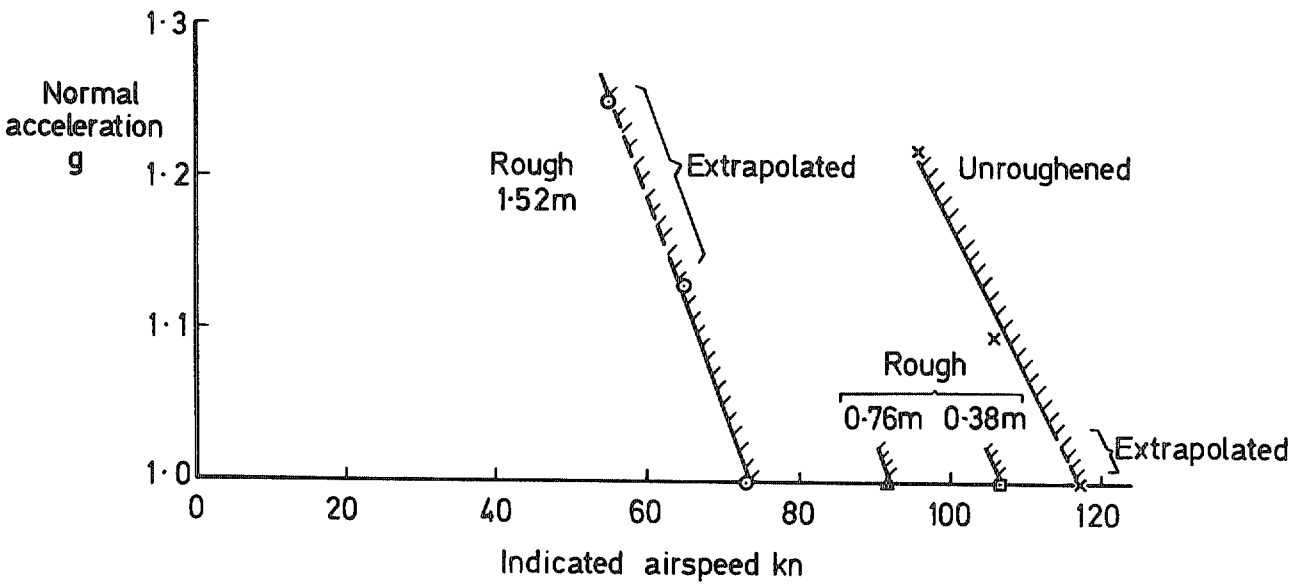

FIG. 12. Effect of blade roughness on $V-g$ boundaries for $\pm 1{\cdot}56$ kN oscillatory pitch link load.

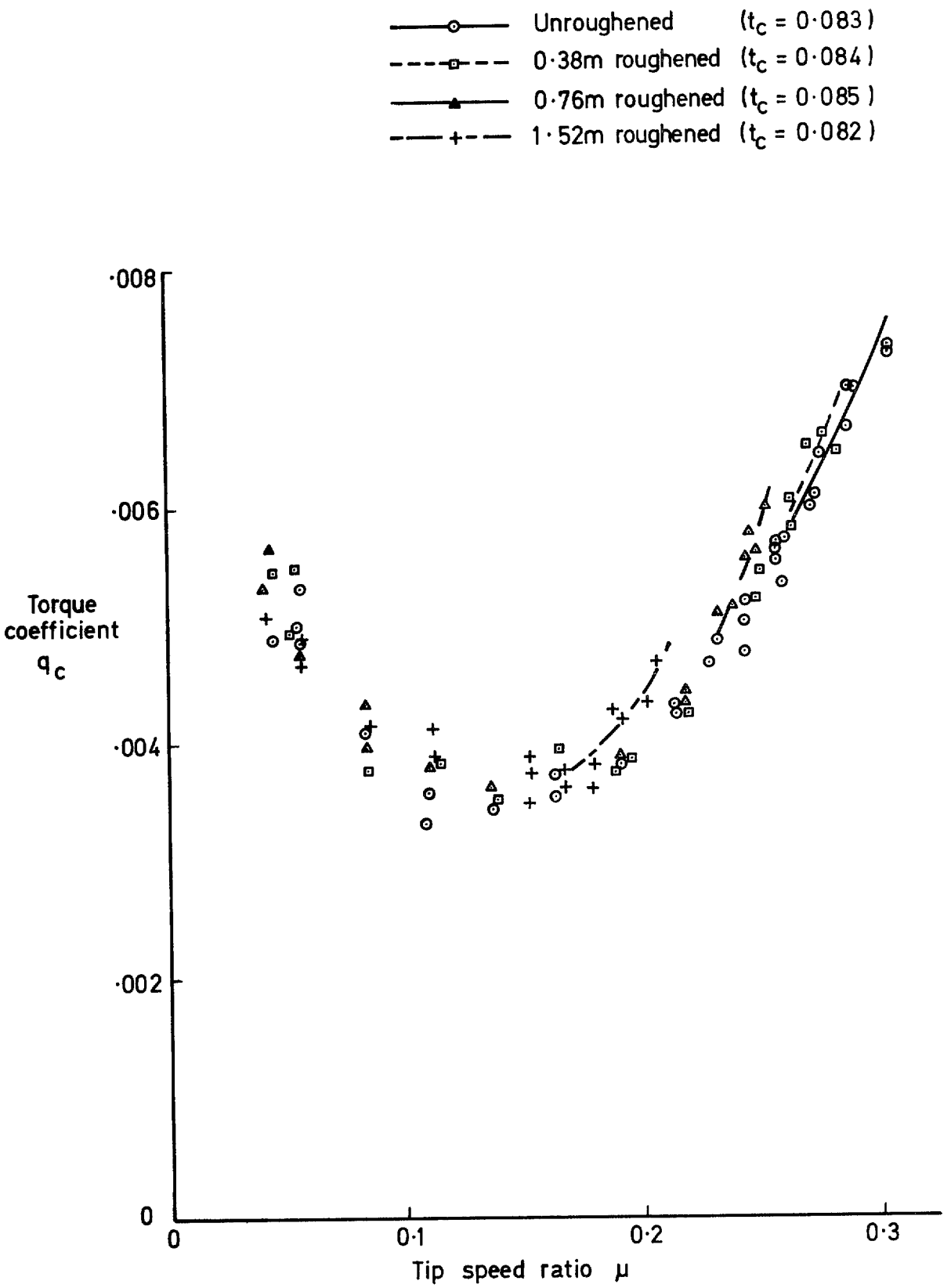

FIG. 13. Effect of roughness on rotor torque required.

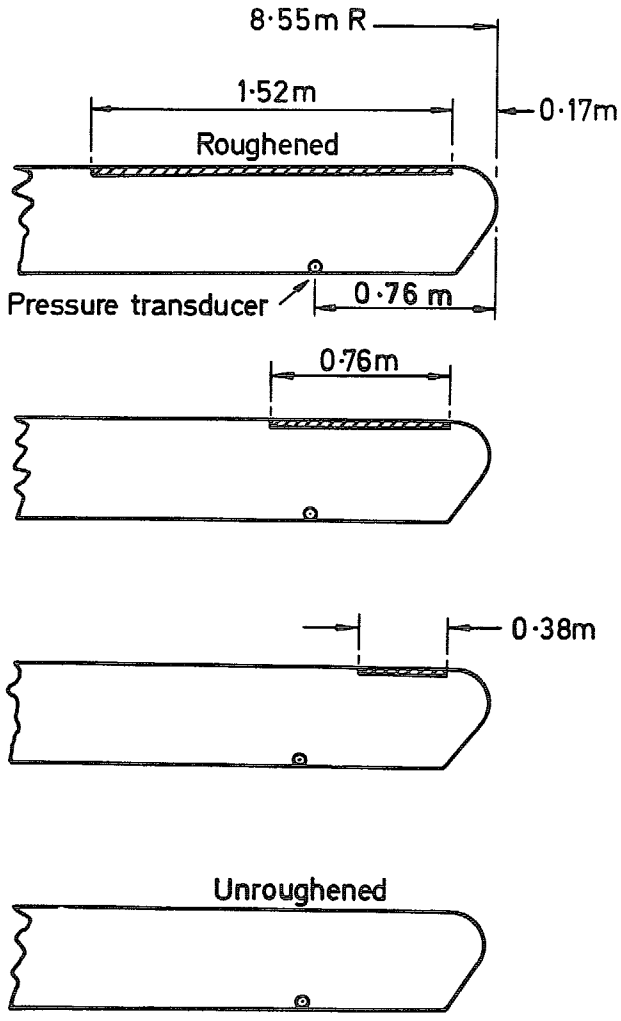

Initial change in character of pitch link load	Pronounced pitch link load oscillation visible	± 1·56kN limit of oscillatory pitch link load	Initial T E pressure divergence
60 kn	73kn	73 kn	60kn
70	85	93	70
85	102	105	100 (Intermittent)
105	110	117	105

FIG. 14. Minimum speed at which changes in load and pressure occurred (excluding near hover).

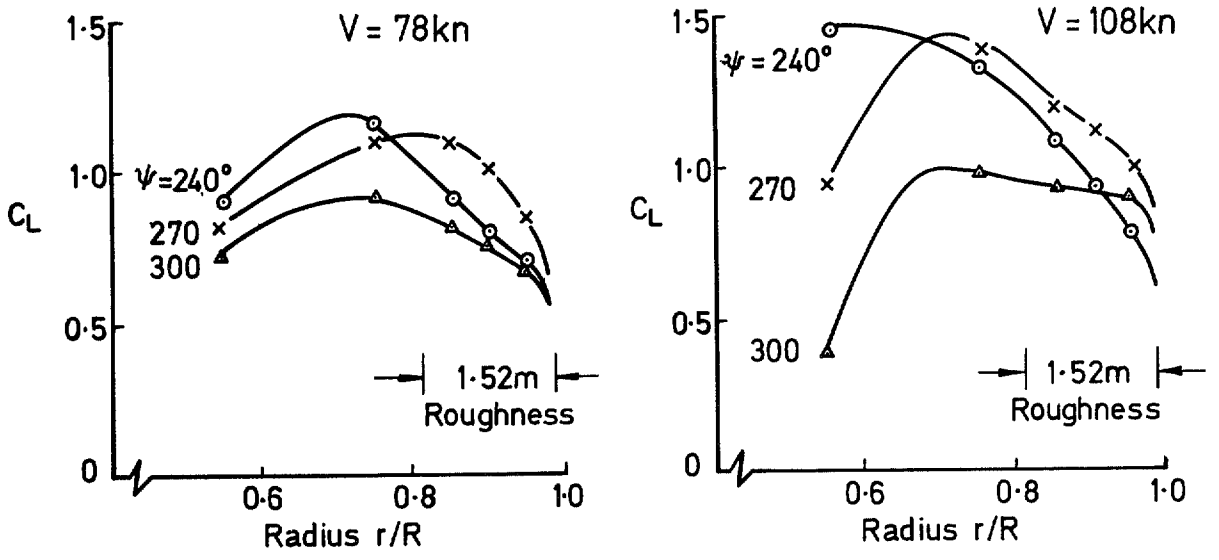

FIG. 15. Tip lift coefficient distributions. Flight tests[4].

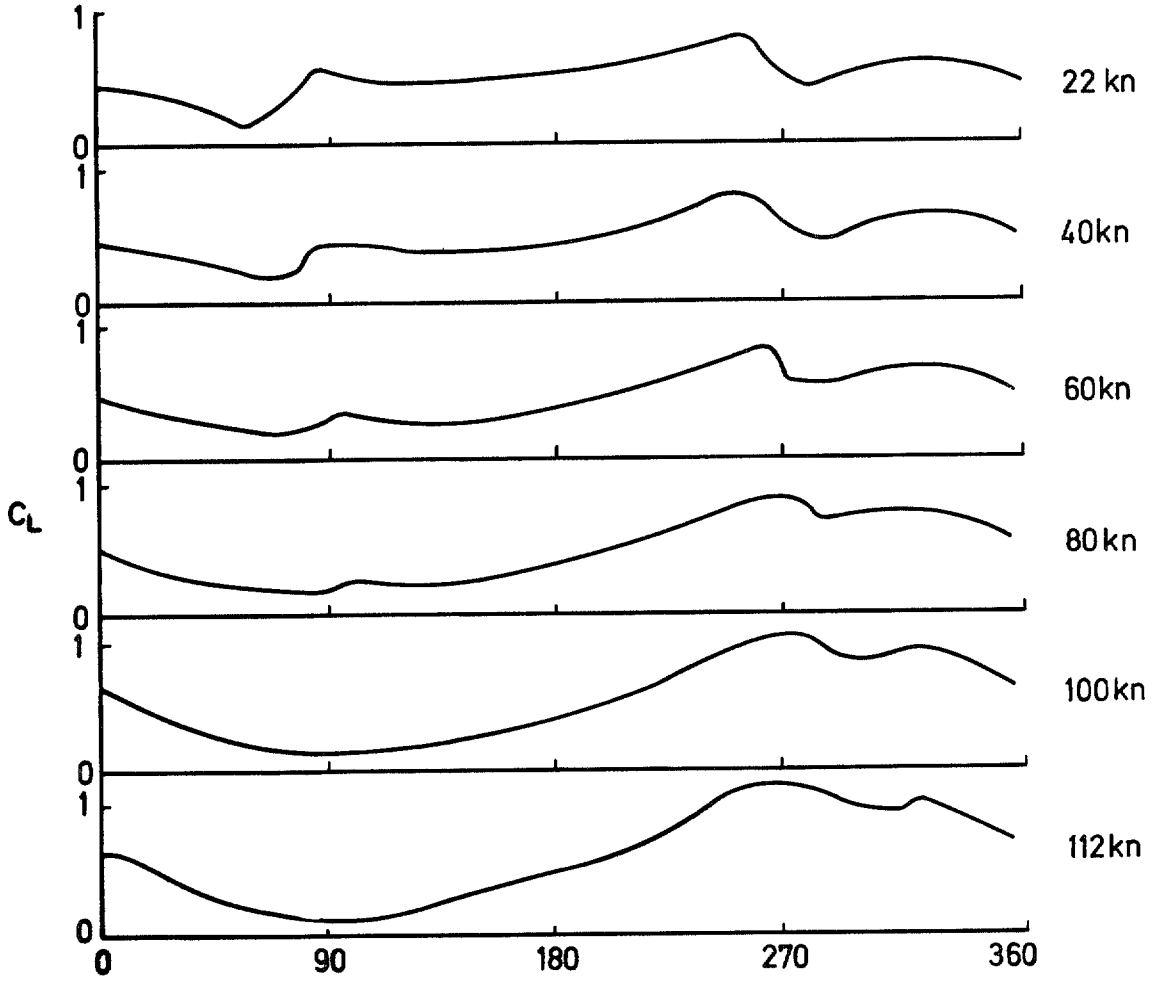

FIG. 16. Variation of lift coefficient with azimuth at 0·91 R. Flight tests[5].

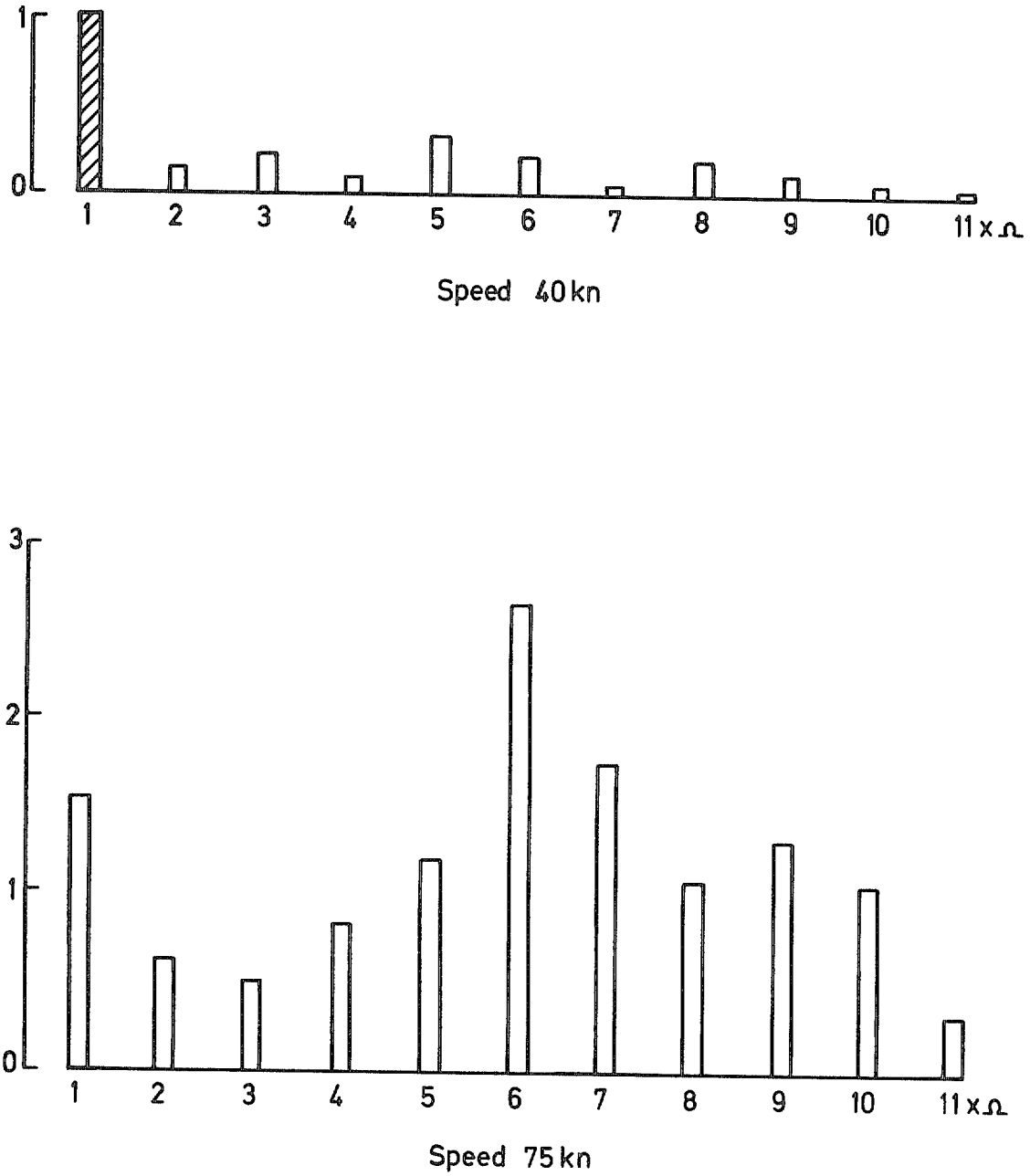

FIG. 17. Pitch link load harmonic amplitudes, normalised with respect to 1st harmonic amplitude at 40 kn (shaded). 1·52 m roughness.

Printed in England for Her Majesty's Stationery Office by J. W. Arrowsmith Ltd., Bristol BS3 2NT
Dd. 587484 K.5. 12/77.

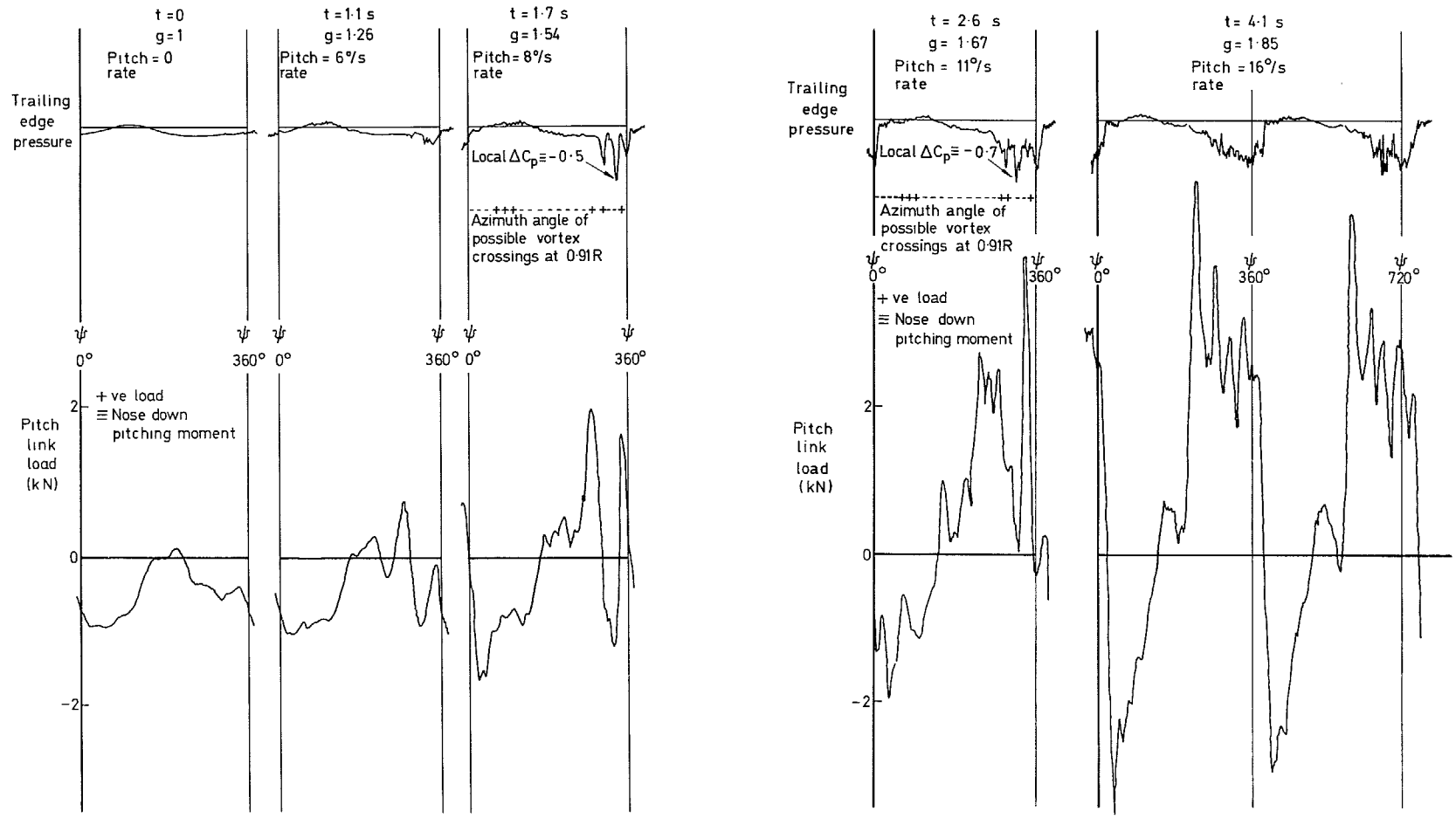

FIG. 18. Time histories of upper surface (0·91C) pressure and pitch link load during a pull-up manoeuvre at 100 kn unroughened.

HER MAJESTY'S STATIONERY OFFICE

Government Bookshops

49 High Holborn, London WC1V 6HB
13a Castle Street, Edinburgh EH2 3AR
41 The Hayes, Cardiff CF1 1JW
Brazennose Street, Manchester M60 8AS
Southey House, Wine Street, Bristol BS1 2BQ
258 Broad Street, Birmingham B1 2HE
80 Chichester Street, Belfast BT1 4JY

Government Publications are also available through booksellers

R. & M. No. 3809

ISBN 0 11 471142 9